

# Compactified holographic conformal order

Alex Buchel

*Department of Physics and Astronomy  
University of Western Ontario  
London, Ontario N6A 5B7, Canada  
Perimeter Institute for Theoretical Physics  
Waterloo, Ontario N2J 2W9, Canada*

## Abstract

We study holographic conformal order compactified on  $S^3$ . The corresponding boundary  $\text{CFT}_4$  has a thermal phase with a nonzero expectation value of a certain operator. The gravitational dual to the ordered phase is represented by a black hole in asymptotically  $AdS_5$  that violates the no-hair theorem. While the compactification does not destroy the ordered phase, it does not cure its perturbative instability: we identify the scalar channel QNM of the hairy black hole with  $\text{Im}[\omega] > 0$ . On the contrary, we argue that the disordered thermal phase of the boundary CFT is perturbatively stable in holographic models of Einstein gravity and scalars.

July 11, 2021

# Contents

<b>1</b>	<b>Introduction</b>	<b>2</b>
<b>2</b>	<b>Summary</b>	<b>5</b>
<b>3</b>	<b>Stability of the holographic CFT disordered thermal states</b>	<b>11</b>
3.1	$\Delta \geq \frac{5}{2}$ . . . . .	14
3.2	$\Delta \in (1, \frac{5}{2})$ . . . . .	15
<b>4</b>	<b>Technical details</b>	<b>15</b>
4.1	$\mathfrak{M}_{PW}^b$ model in the limit $b \rightarrow +\infty$ . . . . .	16
4.2	$\mathfrak{M}_{PW}^b$ model at finite $b$ . . . . .	18
4.3	$\mathfrak{M}_{PW,sym}^b$ model in the limit $b \rightarrow +\infty$ . . . . .	19
<b>A</b>	<b>Hairy black holes and their thermodynamics in <math>\mathfrak{M}_{PW}^b</math> model</b>	<b>20</b>
<b>B</b>	<b><math>h = 0</math> QNMs of the hairy black holes in <math>\mathfrak{M}_{PW}^b</math> model</b>	<b>22</b>
<b>C</b>	<b>Numerical tests</b>	<b>23</b>

## 1 Introduction

*Conformal order* stands for exotic thermal states of conformal theories with spontaneously broken global symmetry group  $G$  [1–4]. For a CFT $_{d+1}$  in Minkowski space-time  $\mathbb{R}^{d,1}$  the existence of the ordered phase implies that there are at least two distinct thermal phases:

$$\frac{\mathcal{F}}{T^{d+1}} = -\mathcal{C} \times \begin{cases} 1, & T^{-\Delta} \langle \mathcal{O}_\Delta \rangle = 0 \implies G \text{ is unbroken;} \\ \kappa, & T^{-\Delta} \langle \mathcal{O}_\Delta \rangle = \gamma \neq 0 \implies G \text{ is spontaneously broken,} \end{cases} \quad (1.1)$$

where  $\mathcal{F}$  is the free energy density,  $T$  is the temperature,  $\mathcal{C}$  is a positive constant proportional to the central charge of the theory, and  $\mathcal{O}_\Delta$  is the order parameter for the symmetry breaking of conformal dimension  $\Delta$ . The parameters  $\kappa$  and  $\gamma$  characterizing the thermodynamics of the the symmetry broken phase are necessarily constants. Note that when  $\kappa > 1$  ( $\kappa < 1$ ), the symmetry broken phase dominates (is subdominant) both in the canonical and the microcanonical ensembles. Irrespectively of the value, provided  $\kappa > 0$ , the symmetry broken phase is thermodynamically stable. It is difficult

to compute directly in a CFT the values  $\{\kappa, \gamma\}$ , thus establishing the present and the (in)stability of the ordered phase. Rather, the authors of [1–4] established the instability of the *disordered* (symmetry preserving) thermal phases in discussed CFTs. The condensation of the identified unstable mode then leads to  $\langle \mathcal{O}_\Delta \rangle \neq 0$  for the new equilibrium thermal state — the conformal order.

Conformal order states are very interesting in the context of holography [5, 6], as they imply the existence of the dual black branes in a Poincare patch of asymptotically  $AdS_{d+2}$  bulk geometry that violate the no-hair theorem. In section 3 we prove a theorem that the disordered conformal thermal states are always stable<sup>1</sup> in dual holographic models of Einstein gravity with multiple scalars. Thus, the mechanism for the conformal order presented in [1] is not viable in these holographic models.

The no-go theorem of section 3 does not imply that the holographic conformal order can not exist. In fact, way before [1], what is now known as a conformal order was constructed in [7]<sup>2</sup>. In the gravitational dual to the holographic conformal order it is straightforward to compute the parameter  $\kappa$  in (1.1), and establish that  $\kappa < 1$ : at best, the holographic conformal order is metastable<sup>3</sup>. In [12] it was established that the holographic conformal order is perturbatively unstable. Specifically, we identified a non-hydrodynamic quasinormal mode (QNM) of the dual hairy black brane with<sup>4</sup>  $\text{Im}[\mathfrak{w}] > 0$ . The purpose of this paper is to use the techniques of [13] to investigate the stability of the holographic conformal order compactified on  $S^3$ .

As introduced, the conformal order is associated with the spontaneous breaking of a global symmetry. Thus, one might wonder whether the order can ever survive the compactification. To this end, we point the following:

- In the infinitely large- $N$  (large central charge) limit spontaneous symmetry breaking can happen on a compact manifold. For a recent example, see a discussion of the spontaneous chiral symmetry breaking of the cascading gauge theory on  $S^3$  [11].
- We present an explicit example in this paper where the existence of the holographic conformal order is not associated with the breaking of any global symmetry.

A detailed summary of our study is provided in section 2. We highlight here the new results:

- Our main model —  $\mathfrak{M}_{PW}^b$  — is a holographic  $CFT_4$  with a single operator  $\mathcal{O}_2$

---

<sup>1</sup>We consider  $AdS_5/CFT_4$  dualities, but the argument can be readily extended to other dimensions.

<sup>2</sup>See [8, 9] for the recent work. Potentially relevant top-down constructions also include [10, 11].

<sup>3</sup>Given the no-go theorem reported here this is not surprising.

<sup>4</sup>We define dimensionless frequencies as  $\mathfrak{w} \equiv w/(2\pi T)$ .

of the conformal dimension  $\Delta = 2$ . The order is associated with the thermal expectation value  $\langle \mathcal{O}_2 \rangle \neq 0$ . The subscript  $_{PW}$  indicates that the model is a deformation,  $b$  is the deformation parameter, of the top-down  $\mathcal{N} = 2^*$  gauge theory/gravity correspondence [14–17].  $\mathcal{N} = 2^*$  holographic correspondence is recovered in the limit  $b \rightarrow 1$ . Importantly, our conformal model  $\mathfrak{M}_{PW}^b$  does not have any global symmetry. We follow the techniques introduced in [9] and construct conformal order in  $\mathfrak{M}_{PW}^b$ , with the holographic boundary CFT in  $\mathbb{R}^{3,1}$  Minkowski space-time, perturbatively as  $b \rightarrow \infty$ . This is the first ever example of the holographic conformal order that is not associated with spontaneous breaking of a global symmetry. We find that  $\kappa < 1$  (see (1.1)) in the model, making the ordered phase not the preferred one. We identify the unstable QNM mode of the dual hairy black brane in asymptotically  $AdS_5$  geometry, and thus establish that the conformal order in  $\mathfrak{M}_{PW}^b$  CFT is unstable.

- We extend  $\mathfrak{M}_{PW}^b$  holographic model when the boundary CFT is compactified on  $S^3$  of a radius  $L$ , equivalently, with the curvature scale  $K = \frac{1}{L^2}$ . We show that the conformal order persists in the limit  $b \rightarrow \infty$  for a wide range of  $\frac{K^{1/2}}{T}$ . The ordered phase is subdominant both the canonical and the microcanonical ensembles. It is always unstable: we identify a QNM mode of the dual hairy black hole in asymptotically  $AdS_5$  geometry with  $\text{Im}[\omega] > 0$ .
- In the limit  $b \rightarrow \infty$ , the ordered and the disordered phases become identical: for the parameters introduced in (1.1), we find  $\kappa(b) - 1 \propto b^{-2} \rightarrow 0$  and  $\gamma(b) \propto b^{-1} \rightarrow 0$ . The absence of the thermodynamically dominant conformal order in  $\mathfrak{M}_{PW}^b$  holographic model in this limit is consistent with the perturbative stability of the disordered phase, as dictated by the general no-go theorem of section 3.
- We study compactified conformal order in  $\mathfrak{M}_{PW}^b$  model at finite  $b$  for select values of  $\frac{K^{1/2}}{T}$ . We establish that the conformal order exists only for  $b > b_{crit}(K)$ . Since  $b_{crit}$  is found to be always larger than 1, the holographic model  $\mathfrak{M}_{PW}^b$  with the ordered phase is always a deformation of the  $\mathcal{N} = 2^*$ /Pilch-Warner top-down holography. In other words, similar to [9], there is no conformal order in  $\mathcal{N} = 2^*$  theory.
- We establish the compactified conformal order in  $\mathfrak{M}_{PW}^b$  model at finite  $b$ , when it exists, is thermodynamically subdominant and unstable.

- It is easy to 'symmetrize' the holographic model  $\mathfrak{M}_{PW}^b$ : the resulting  $\mathfrak{M}_{PW,sym}^b$  model has a  $\mathbb{Z}_2$  parity symmetry  $\mathcal{O}_2 \leftrightarrow -\mathcal{O}_2$ . In  $\mathfrak{M}_{PW,sym}^b$  model, the compactified conformal order is associated with the spontaneous breaking of this parity invariance. All the features of this symmetric model are qualitatively identical to those of  $\mathfrak{M}_{PW}^b$  model.

We finish the introduction with the comment about the prospect for constructing the thermodynamically dominant and stable holographic conformal order. All the known constructions of the holographic conformal order [7–9], as well as the models discussed here, can be thought to rely on a perturbative deformation of the disordered phase in the holographic CFTs. The no-go theorem of section 3 strongly suggests that one can never construct a thermodynamically dominant phase in this fashion — again we stress the difference here with the QFT approaches of [1–4]. So, if the stable holographic conformal order exists, it must be discontinuous, in some sense, from the disordered phase. The possible examples could be Klebanov-Strassler black branes/black holes [10, 11] in the limit of infinitely high temperature  $\frac{T}{\Lambda} \rightarrow \infty$ , where  $\Lambda$  is the strong coupling scale of the boundary cascading gauge theory. A big *if* is the existence of these black branes/black holes in the high temperature limit in the supergravity approximation. We expect to report on this question in the near future.

## 2 Summary

The starting point of our analysis is an example of the gauge theory/string theory holographic correspondence between  $\mathcal{N} = 2^* SU(N)$  theory (in the planar limit and at large 't Hooft coupling) and type IIB supergravity [14–17]. The corresponding bulk effective action resulting from the dimensional reduction on the five-sphere of ten-dimensional supergravity takes form

$$S_5 = \frac{1}{16\pi G_5} \int_{\mathcal{M}_5} d^5\xi \sqrt{-g} \left[ R - 12(\partial\alpha)^2 - 4(\partial\chi)^2 - V(\alpha, \chi) \right], \quad (2.1)$$

with the potential  $V$  determined from the superpotential  $W$  as

$$V = \frac{1}{4} \left( \frac{1}{3} \left( \frac{\partial W}{\partial \alpha} \right)^2 + \left( \frac{\partial W}{\partial \chi} \right)^2 \right) - \frac{4}{3} W^2, \quad W = -e^{-2\alpha} - \frac{1}{2} e^{4\alpha} \cosh(2\chi). \quad (2.2)$$

The bulk scalars  $\alpha$  and  $\chi$  are (correspondingly) the holographic dual to operators  $\mathcal{O}_2$  and  $\mathcal{O}_3$  of the  $\mathcal{N} = 4$  Yang-Mills [15, 18, 19]. Finally, five-dimensional Newton's

constant  $G_5$  is<sup>5</sup>

$$G_5 = \frac{4\pi}{N^2}. \quad (2.3)$$

The non-normalizable coefficients of the bulk scalars  $\alpha$  and  $\chi$  are related to the masses of the bosonic and fermionic components of  $\mathcal{N} = 2$  hypermultiplet. In this paper we are interested in *conformal* theories, thus, these parameters are set to zero. To simplify the discussion, we can consistently set  $\chi \equiv 0$ , leading to a conformal model  $\mathfrak{M}_{PW} — \mathcal{N} = 4 SU(N)$  SYM with a single operator  $\mathcal{O}_2$  of dimension  $\Delta = 2$ :

$$V_{\mathfrak{M}_{PW}} = -2e^{2\alpha} - e^{-4\alpha}. \quad (2.4)$$

Note that  $\mathfrak{M}_{PW}$  does not have any global symmetry. It does not have a conformal order either, as we already alluded to in section 1. Following [9], we generate a class of deformed conformal models  $\mathfrak{M}_{PW}^b$ , with

$$\begin{aligned} V_{\mathfrak{M}_{PW}^b} &= -3 - 12\alpha^2 + b \left( 3 + 12\alpha^2 - 2e^{2\alpha} - e^{-4\alpha} \right) \\ &= -3 - 12\alpha^2 + 8b \alpha^3 + b \mathcal{O}(\alpha^4). \end{aligned} \quad (2.5)$$

Note that

$$\lim_{b \rightarrow 1} V_{\mathfrak{M}_{PW}^b} = V_{\mathfrak{M}_{PW}}, \quad (2.6)$$

*i.e.*, we recover in this limit the top-down holographic model  $\mathfrak{M}_{PW}$ . We find that there is a thermal ordered phase in  $\mathfrak{M}_{PW}^b$ , provided  $b > b_{crit} > 1$ . The precise value of  $b_{crit}$  below which the ordered phase ceases to exist depends on  $K^{1/2}/T$ , *i.e.*, the ratio of the  $S^3$  compactification scale and the temperature  $T$ .

In the rest of this section we explain the results only; a curious reader can find technical details necessary to reproduce them in section 4.

In fig. 1 we present the results for the conformal order in  $\mathfrak{M}_{PW}^b$  model in the limit  $b \rightarrow +\infty$  for different values of  $K^{1/2}/T$ . Note that the thermal expectation value  $\langle \mathcal{O}_2 \rangle \propto \frac{1}{b}$  (the left panel), implying that the backreaction of the bulk scalar  $\alpha$  on the geometry becomes vanishingly small in the limit  $b \rightarrow +\infty$ . Constructed conformal order is perturbatively unstable: in the right panel we identify a QNM of the corresponding hairy black hole with  $\text{Im}[\omega] > 0$ . The disordered phase is represented holographically by  $AdS_5$  black hole. There are four distinct regimes of  $K^{1/2}/T$  in the disordered phase, which we also highlighted with solid/dashed/dotted curves in the

---

<sup>5</sup>We set the asymptotic  $AdS_5$  curvature radius to 2.

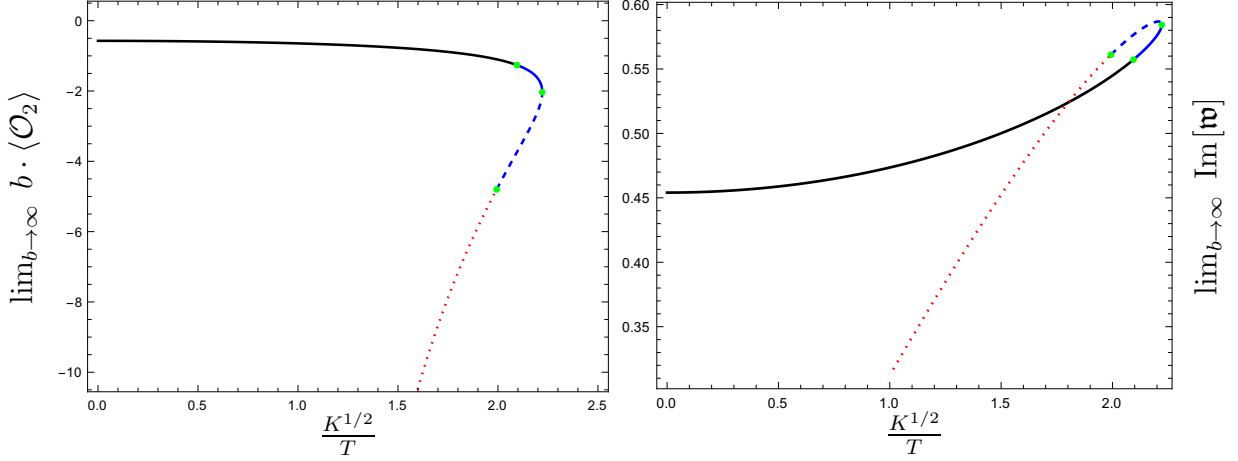


Figure 1: The left panel: the thermal expectation value of the order parameter  $\mathcal{O}_2$  of the conformal model  $\mathfrak{M}_{PW}^b$  in the limit  $b \rightarrow +\infty$  as a function of  $\frac{K^{1/2}}{T}$ . The right panel: the unstable QNM of the hairy black hole representing the holographic dual to the ordered phase.

ordered phase:

- the solid black curves correspond to

$$0 < \frac{K^{1/2}}{T} < \frac{2\pi}{3}, \quad (2.7)$$

with  $AdS_5$  black holes temperature about the Hawking-Page transition [20, 21];

- the solid blue curves correspond to

$$\frac{2\pi}{3} < \frac{K^{1/2}}{T} < \frac{\pi}{\sqrt{2}}, \quad (2.8)$$

with  $AdS_5$  black holes temperature below the Hawking-Page transition, but having a positive specific heat;

- the dashed blue curves correspond to

$$1.993(4) < \frac{K^{1/2}}{T} < \frac{\pi}{\sqrt{2}}, \quad (2.9)$$

with  $AdS_5$  black holes having a negative specific heat, but being perturbatively stable with respect to localization on  $S^5$  [22, 23];

- the dotted red curves correspond to

$$\frac{K^{1/2}}{T} < 1.993(4), \quad (2.10)$$

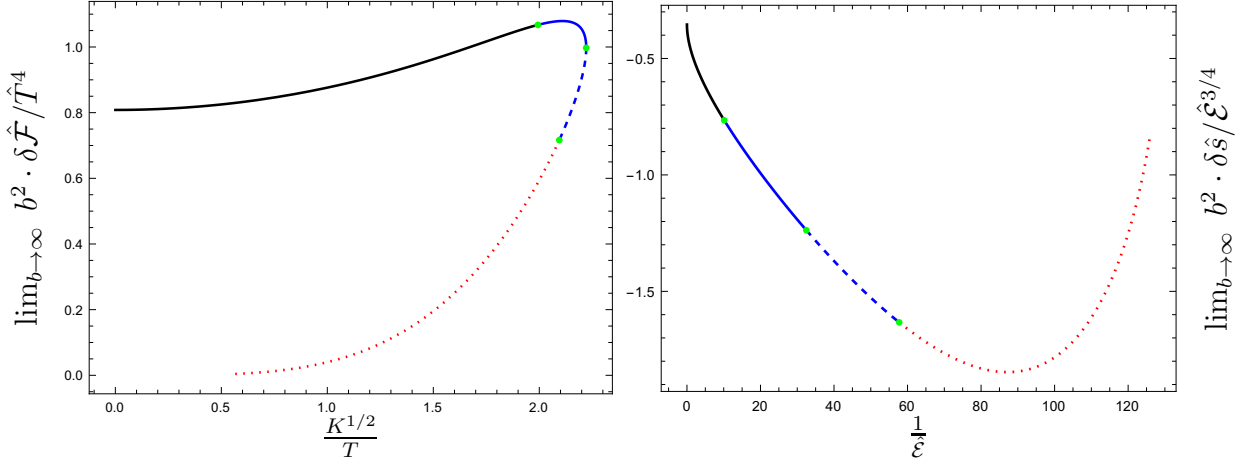


Figure 2: The ordered phase of the conformal model  $\mathfrak{M}_{PW}^b$  in the limit  $b \rightarrow +\infty$  has a higher free energy density than that of the disordered phase at the corresponding temperature (the left panel). The ordered phase of the conformal model  $\mathfrak{M}_{PW}^b$  in the limit  $b \rightarrow +\infty$  has a lower entropy density than that of the disordered phase at the corresponding energy density (the right panel). See (2.11) and (2.12) for the definition of the reduced thermodynamic functions.

with  $AdS_5$  black holes being perturbatively unstable with respect to localization on  $S^5$ .

In fig. 2 we show that the ordered phase of the conformal model  $\mathfrak{M}_{PW}^b$  in the limit  $b \rightarrow +\infty$  is subdominant both in the canonical ensemble (the left panel) and the microcanonical ensemble (the right panel). We define the reduced free energy density  $\hat{\mathcal{F}}$ , the reduced energy density  $\hat{\mathcal{E}}$ , the reduced entropy density  $\hat{s}$ , and the reduced temperature  $\hat{T}$  as<sup>6</sup>

$$\hat{\mathcal{F}} \equiv \frac{8}{\pi^2 N^2} \frac{\mathcal{F}}{K^2}, \quad \hat{\mathcal{E}} \equiv \frac{8}{\pi^2 N^2} \frac{\mathcal{E}}{K^2}, \quad \hat{s} \equiv \frac{8}{\pi^2 N^2} \frac{s}{K^{3/2}}, \quad \hat{T} = \frac{T}{K^{1/2}}, \quad (2.11)$$

furthermore,

$$\delta \hat{\mathcal{F}} \equiv \hat{\mathcal{F}}_{ordered} - \hat{\mathcal{F}}_{disordered} \Big|_{\text{fixed } \hat{T}}, \quad \delta \hat{s} \equiv \hat{s}_{ordered} - \hat{s}_{disordered} \Big|_{\text{fixed } \hat{\mathcal{E}}}. \quad (2.12)$$

The color/style coding in the left panel is as in fig. 1; in the right panel the coding reflects the values of  $\hat{\mathcal{E}}$  of the disordered phase corresponding to (2.7)-(2.10).

<sup>6</sup>The normalization is chosen so that  $\lim_{\hat{T} \rightarrow \infty} \frac{\hat{\mathcal{F}}}{\hat{T}^4} = -1$ .



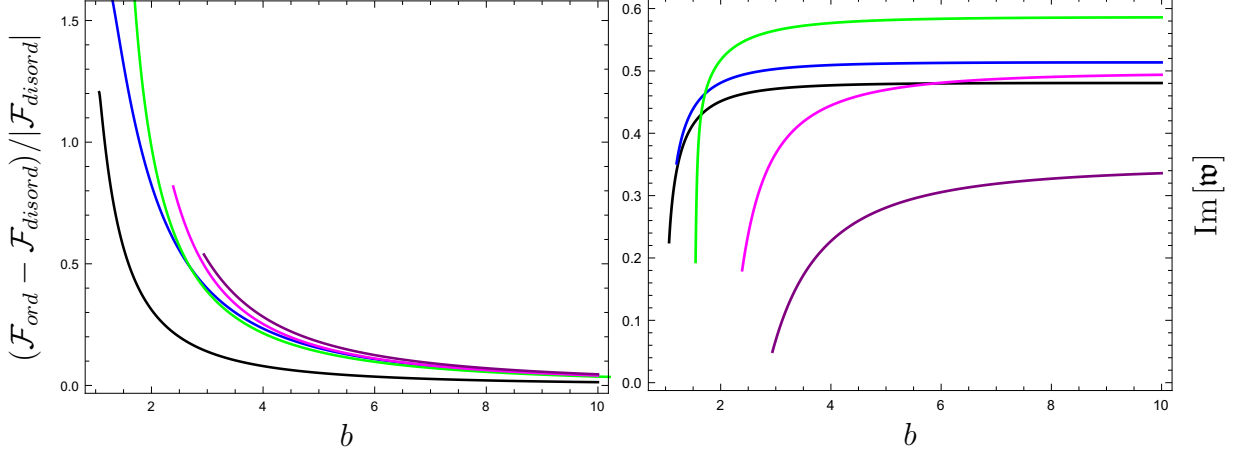


Figure 3: The ordered phase of the conformal model  $\mathfrak{M}_{PW}^b$  at finite  $b$  and select values of  $K^{1/2}/T$ , see (2.13). The left panel demonstrates that the ordered phase has a higher free energy density than that of the disordered phase (at the corresponding temperature). The right panel identifies the QNM in hairy black holes, holographically dual to the ordered phase, with  $\text{Im}[\mathfrak{w}] > 0$ , rendering this thermal ordered phase perturbatively unstable.

In fig. 3 we present the results for the thermal ordered phase in  $\mathfrak{M}_{PW}^b$  model for finite values of  $b$  and select values of  $\frac{K^{1/2}}{T}$ :

$$\frac{K^{1/2}}{T} \approx \frac{\pi}{\sqrt{2}} \left\{ \frac{1}{2}, \frac{3}{4}, 1, \frac{3}{4}, \frac{1}{2} \right\}. \quad (2.13)$$

The black and the blue curves represent black holes with the positive specific heat; the magenta and the purple curves represent black holes with the negative specific heat. The left panel indicates that the disordered phase has a lower free energy density, and thus is the preferred one<sup>7</sup>. The right panel demonstrates that the ordered phase is perturbatively unstable: we identify the quasinormal mode in the helicity zero sector of the dual hairy black hole with  $\text{Im}[\mathfrak{w}] > 0$ .

Thermal ordered phases in  $\mathfrak{M}_{PW}^b$  model exist only for  $b > b_{crit}$ . In fig. 4 we present the estimate for  $b_{crit}$  for the set of  $K^{1/2}/T$  in (2.13). Additionally, the red dot indicates (see fig. 8)

$$b_{crit} \Big|_{K=0} \approx 1.000(1). \quad (2.14)$$

<sup>7</sup>The disordered phase is also the dominant one in the microcanonical ensemble.

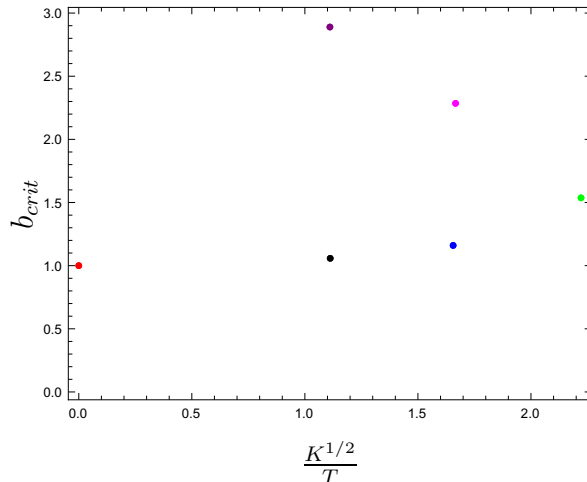


Figure 4: Thermal ordered phases in  $\mathfrak{M}_{PW}^b$  model exist only for  $b > b_{crit}$ .  $b_{crit}$  is estimated for the set of  $K^{1/2}/T$  in (2.13). The red dot represents  $b_{crit}(K = 0)$ .

The fact that  $b_{crit} > 1$  implies that there is no thermal ordered phase in top-down holographic model  $\mathfrak{M}_{PW}$ .

So far we presented the evidence that the holographic conformal order survives the compactification of the dual boundary theory on  $S^3$ , but remains unstable. In the example presented, the order was not associated with the spontaneous breaking of any global symmetry. The reader might reasonable worry whether our conclusions are specific to models without any global symmetry. Rather, we claim that our results are generic: we extend analysis to  $\mathfrak{M}_{PW,sym}^b$  model, where the bulk scalar potential is  $\mathbb{Z}_2$ -symmetric,

$$\begin{aligned} V_{\mathfrak{M}_{PW,sym}^b} &= \frac{1}{2} V_{\mathfrak{M}_{PW}^b}(\alpha) + \frac{1}{2} V_{\mathfrak{M}_{PW}^b}(-\alpha) \\ &= -3 - 12\alpha^2 - 12b\alpha^4 - b\mathcal{O}(\alpha^6), \end{aligned} \quad (2.15)$$

and the conformal order is associated with the spontaneous breaking of this parity invariance. In fig. 5 we present the results for the conformal order in  $\mathfrak{M}_{PW,sym}^b$  model in the limit  $b \rightarrow +\infty$  for different values<sup>8</sup> of  $K^{1/2}/T$ . The left panel shows the order parameter  $\langle \mathcal{O}_2 \rangle \propto \pm \frac{1}{\sqrt{b}}$ , and the right panel identifies an unstable QNM of the corresponding hairy black hole. The finite  $b$  results of  $\mathfrak{M}_{PW,sym}^b$  model are qualitatively identical to those of  $\mathfrak{M}_{PW}^b$  model.

---

<sup>8</sup>The color/style coding is as in fig. 1.

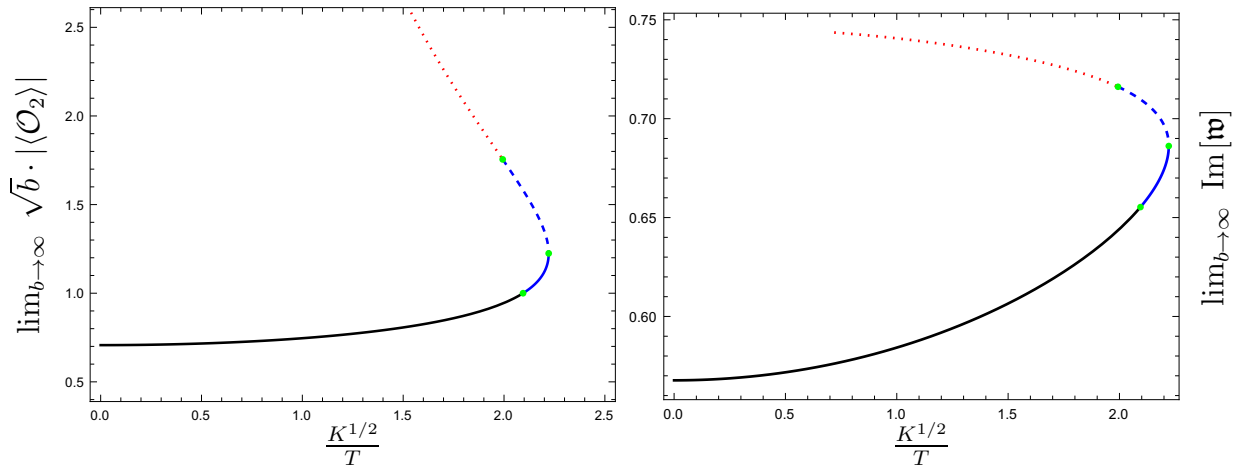


Figure 5: The left panel: the thermal expectation value of the order parameter  $\mathcal{O}_2$  of the conformal model  $\mathfrak{M}_{PW,sym}^b$  in the limit  $b \rightarrow +\infty$  as a function of  $\frac{K^{1/2}}{T}$ . The right panel: the unstable QNM of the hairy black hole representing the holographic dual to the ordered phase.

### 3 Stability of the holographic CFT disordered thermal states

In this section we prove that disordered phases of four-dimensional holographic CFTs on  $\mathbb{R}^3$  or  $S^3$ , dual to bulk models of asymptotically  $AdS_5$  Einstein gravity with arbitrary scalars, are perturbatively stable. These disordered phases are represented by AdS-Schwarzschild black branes/black holes. It is well-known that AdS-Schwarzschild black branes/black holes are stable with respect to the purely gravitational perturbations [24] — we extend this statement to the stability with respect to the bulk scalar fluctuations.

It is important to stress what potential instabilities are not covered by the analysis below. A top-down conformal holographic model is formulated in ten dimensional type IIB supergravity in asymptotically  $AdS_5 \times \mathcal{V}_5$ , where  $\mathcal{V}_5$  is a compact manifold,  $\mathcal{V}_5 = S^5$  in the familiar example of large- $N$   $\mathcal{N} = 4$  SYM. It is known that  $AdS_5$ -Schwarzschild black holes can be unstable with respect to metric fluctuations carrying nonzero momentum on  $\mathcal{V}_5$  [22, 23, 25]. Once we reduce the ten-dimensional holographic correspondence on  $\mathcal{V}_5$  we lose access to such fluctuations. However, such instabilities are incorrect to interpret as Schwarzschild black holes growing the scalar hair and violating the no-hair theorem. Rather, these are the instabilities of the initially smeared over  $\mathcal{V}_5$  black holes towards localization on the compact transverse space.

Consider a holographic correspondence encoded in an effective five-dimensional

gravitational action

$$S_5 = \frac{1}{16\pi G_5} \int_{\mathcal{M}_5} d^5\xi \sqrt{-g} \left[ R - \frac{1}{2} \sum_{j=1}^p (\partial\phi_j)^2 - V(\{\phi_j\}) \right]. \quad (3.1)$$

We will keep the scalar potential  $V(\{\phi_j\})$  arbitrary, in particular, we will not assume any global symmetries in the model<sup>9</sup>. To conform with the rest of the discussion in this paper, we set the radius of the asymptotically  $AdS_5$  geometry to 2, then, the potential takes form

$$V(\{\phi_j\}) = -3 - \frac{1}{2} \sum_{i,j=1}^p m_{ij} \phi_i \phi_j + \mathcal{O}(\phi^3). \quad (3.2)$$

The disordered phase is the  $AdS_5$ -Schwarzschild black brane/black hole, which we write in infalling Eddington-Finkelstein (EF) coordinates as (compare with (A.1))

$$ds_5^2 = -c_1^2 d\tau^2 - 2c_1 c_3 d\tau dr + c_2^2 d\Omega_{(3,K)}^2, \quad (3.3)$$

where  $\tau$  is the EF time, and the minus sign in  $d\tau dr$  term is due to the fact that the AdS boundary is at  $r \rightarrow 0$ , with

$$c_1 = \frac{f^{1/2}}{r h^{1/4}}, \quad c_2 = \frac{1}{r h^{1/4}}, \quad c_3 = \frac{h^{1/4}}{r f^{1/2}}, \quad (3.4)$$

$$f = \frac{(2r+1)(16Kr^2 + 2r^2 + 2r + 1)}{(r+1)^4}, \quad h = \frac{16}{(1+r)^4}.$$

Additionally, the background values of all the scalars are set to zero

$$\phi_j(r) \equiv 0. \quad (3.5)$$

Following [13], there are  $p+3$  branches of the QNMs:

- helicity  $h=2$  and  $h=1$  branches of the metric fluctuations;
- $p+1$  branches of the helicity  $h=0$  fluctuations.

$h=2$  and  $h=1$  branches can not contain instabilities [13, 24], thus we focus on the helicity  $h=0$  fluctuations. Because the scalar fields vanish in the background (3.5), (the stable [24]) helicity  $h=0$  metric fluctuations will decouple from the fluctuations of the bulk scalars (see eq.(A.22) of [13]). Moreover, for the same reason, generically coupled  $p$  branches of the scalar fluctuations will depend only on the mass-matrix coefficients  $m_{ij}$  in the potential (3.2), and not on the details of nonlinearities  $\mathcal{O}(\phi^3)$

---

<sup>9</sup>We explain shortly how the unitarity of the boundary  $CFT_4$  constrains this potential.

(see eq.(A.23) of [13]). Thus, for all practical purposes we can truncate the generic scalar potential in (3.2) to  $\mathcal{O}(\phi^2)$ . Using the orthogonal rotation in the field space, the equivalent to (3.1) effective action (in regards to computing the spectra of the QNMs) is given by

$$S_5 = \frac{1}{16\pi G_5} \int_{\mathcal{M}_5} d^5\xi \sqrt{-g} \left[ R + 3 - \frac{1}{2} \sum_{j=1}^p \left\{ (\partial\chi_j)^2 + \mu_j^2 \chi_j^2 \right\} \right], \quad (3.6)$$

with a new scalar  $\chi_j$  of mass  $\mu_j^2$  dual to an operator  $\mathcal{O}_j$  of dimension  $\Delta_j$  of the boundary CFT

$$\{\mathcal{O}_j, \Delta_j\} \iff \{\chi_j, 4\mu_j^2 = \Delta_j(\Delta_j - 4)\}, \quad \Delta_j > 1. \quad (3.7)$$

In (3.7) we assumed the Breitenlohner-Freedman bound [26] on the scalar masses, equivalently the unitarity bound on the operators of the interactive boundary CFT [27]. An advantage of using (3.6) is that the branches of the scalar fluctuations  $\Phi_j$  now completely decouple:

$$0 = \square \Phi_j - \mu_j^2 \Phi_j = \square \Phi_j - \frac{\Delta_j(\Delta_j - 4)}{4} \Phi_j, \quad j = 1, \dots, p. \quad (3.8)$$

QNM equations (3.8) are solved with the regularity condition at the horizon, and the boundary fall-off

$$\Phi_j \sim r^{\Delta_j}, \quad r \rightarrow 0. \quad (3.9)$$

Each of the  $p$  QNM branches can be analyzed separately: from now on we drop the subscript  $j$  and consider  $\Delta$  to be continuous with  $\Delta > 1$ .

The argument below is standard in the literature [28] — we are simply being careful with the various boundary terms. Introduce

$$\Phi = e^{-iw\tau} \frac{S(\Omega_{3,K})}{c_2^{3/2}} \psi(r), \quad \text{where} \quad \Delta_{\Omega_{3,K}} S + k^2 S = 0. \quad (3.10)$$

From (3.8) we find the second order equation for  $\psi$ :

$$0 = \mathcal{X} \equiv \left[ \frac{c_1}{c_3} \psi' \right]' + 2i w \psi' - c_1 c_3 V(r) \psi, \quad (3.11)$$

where using (3.4) we explicitly evaluate  $V$  as

$$V = \frac{3r^2(4r^2 + 2r + 1)K}{(r+1)^4} + \frac{4k^2 r^2}{(r+1)^2} + \frac{9r^4}{16(r+1)^4} + \frac{(2\Delta - 3)(2\Delta - 5)}{16}, \quad (3.12)$$

with

$$k^2 = \begin{cases} [0, +\infty), & \text{if } K = 0; \\ K\ell(\ell + 2), \ell \in \mathbb{Z}_+, & \text{if } K > 0. \end{cases} \quad (3.13)$$

Eq. (3.11) needs to be solved subject to the boundary conditions

$$\begin{aligned} \text{UV :} \quad & \psi = r^{\Delta-3/2} (1 + \mathcal{O}(r)), \quad r \rightarrow 0, \\ \text{IR :} \quad & \psi = \mathcal{O}(1), \quad y \equiv \frac{1}{r} \rightarrow 0. \end{aligned} \quad (3.14)$$

In general, the solution of (3.11) results in complex  $\psi$  and  $w$ .

We present an analytic argument that  $\text{Im}[\mathfrak{w}] < 0$  when  $\Delta \geq \frac{5}{2}$ ; for  $\Delta \in (1, \frac{5}{2})$  we need to resort to numerics. Establishing  $\text{Im}[\mathfrak{w}] < 0$  implies stability of the disordered phases of holographic CFTs with the effective action (3.1). Note in particular that  $\mathfrak{M}_{PW}^b$  and  $\mathfrak{M}_{PW, sym}^b$  models discussed in section 2 are the special cases of (3.1).

### 3.1 $\Delta \geq \frac{5}{2}$

Note that in this case the potential  $V$  (3.11) is manifestly positive for  $r \in (0, \infty)$ . Assuming  $\{\psi, w\}$  is a solution to (3.11), we define

$$0 = \mathcal{I}(\epsilon, y_h) = - \int_{r=\epsilon}^{r=1/y_h} dr \mathcal{X} \bar{\psi}. \quad (3.15)$$

Ultimately, we will take the limit

$$0 = \lim_{(\epsilon, y_h) \rightarrow 0} \mathcal{I}(\epsilon, y_h) \equiv \mathcal{I}. \quad (3.16)$$

Using the explicit definition of  $\mathcal{X}$  (3.11) and integrating by parts,

$$\mathcal{I}(\epsilon, y_h) = \underbrace{-\bar{\psi} \frac{c_1}{c_3} \psi' \Big|_{r=\epsilon}^{r=1/y_h}}_{\text{bt}} + \underbrace{\int_{\epsilon}^{1/y_h} \left\{ \frac{c_1}{c_3} |\psi'|^2 + c_1 c_3 V |\psi|^2 \right\} dr}_{\mathcal{J}(\epsilon, y_h)} - \underbrace{2i w \int_{\epsilon}^{1/y_h} \psi' \bar{\psi} dr}_{\mathcal{H}(\epsilon, y_h)}. \quad (3.17)$$

Note that  $\mathcal{J}(\epsilon, y_h)$  is manifestly positive, and the boundary term bt vanishes in the limit  $(\epsilon, y_h) \rightarrow 0$

$$\begin{aligned} \text{UV :} \quad & \bar{\psi} \frac{c_1}{c_3} \psi' \Big|_{r=\epsilon} \propto \left( \Delta - \frac{3}{2} \right) \epsilon^{2\Delta-4} \rightarrow 0 \quad \text{since} \quad \Delta \geq \frac{5}{2}, \\ \text{IR :} \quad & \bar{\psi} \frac{c_1}{c_3} \psi' \Big|_{r=1/y_h} \propto y_h \rightarrow 0. \end{aligned} \quad (3.18)$$

Thus

$$0 = \mathcal{I} = \mathcal{J} - 2i\mathcal{H} \quad \Longrightarrow \quad \text{Re}[\mathcal{H}] = 0, \quad (3.19)$$

leading to

$$\begin{aligned} 0 &= \int_0^{+\infty} \left\{ w\psi'\bar{\psi} + \bar{w}\bar{\psi}'\psi \right\} dr = (w - \bar{w}) \int_0^{+\infty} \psi'\bar{\psi} dr + \bar{w} \left| \psi \right|^2 \Big|_{r=0}^{r \rightarrow \infty} \\ &= (w - \bar{w}) \int_0^{+\infty} \psi'\bar{\psi} dr + \bar{w} |\psi_h|^2 \quad \Longrightarrow \quad \mathcal{H} = \frac{|w|^2}{-2i\text{Im}[w]} |\psi_h|^2, \end{aligned} \quad (3.20)$$

where we integrated the second term by parts and dropped in the second line the  $r \rightarrow 0$  boundary term since  $|\psi|^2 \propto r^{2\Delta-3} \rightarrow 0$ . From (3.19) we find then

$$\int_0^{+\infty} \left\{ \frac{c_1}{c_3} |\psi'|^2 + c_1 c_3 V |\psi|^2 \right\} dr = -\frac{|w|^2}{\text{Im}[w]} |\psi_h|^2 \quad \Longrightarrow \quad \text{Im}[\mathfrak{w}] < 0. \quad (3.21)$$

### 3.2 $\Delta \in (1, \frac{5}{2})$

The analytic proof of section 3.1 fails here since:

- the potential  $V$  (3.12) can be negative for small  $r$  when  $\Delta \in (\frac{3}{2}, \frac{5}{2})$ ;
- the UV boundary term in (3.18) does not vanish for  $\Delta \leq 2$ ;
- the UV boundary term in (3.20) does not vanish for  $\Delta \leq \frac{3}{2}$ .

Note that our models  $\mathfrak{M}_{PW}^b$  and  $\mathfrak{M}_{PW,sym}^b$  (and in particular the top-down example  $\mathfrak{M}_{PW}$ ) have disordered phase with  $\Delta = 2$ . We will not attempt to find an analytic proof that  $\text{Im}[\mathfrak{w}] < 0$  when  $\Delta \in (1, \frac{5}{2})$ , and instead present numerical evidence that this is indeed the case.

In fig. 6 we present  $\text{Re}[\mathfrak{w}]$  (the left panel) and  $\text{Im}[\mathfrak{w}]$  (the right panel) of the lowest  $\Delta = 2$  QNMs in the disordered phase with  $\ell = 0$  (black curves),  $\ell = 1$  (blue curves) and  $\ell = 2$  (purple curves). The vertical grey line indicates the Hawking-Page transition of the  $AdS_5$  Schwarzschild black hole; the cyan line indicates the terminal temperature (the dashed/dotted black holes have a negative specific heat), and the red line indicates the onset of the localization instability of the  $AdS_5 \times S^5$  Schwarzschild black holes.

In fig. 7 we present  $\text{Re}[\mathfrak{w}]$  (the left panel) and  $\text{Im}[\mathfrak{w}]$  (the right panel) of the lowest  $\ell = 0$  QNMs in the disordered phase with  $\Delta \in (1, \frac{5}{2})$ .

## 4 Technical details

In this section we highlight technical details useful to reproduce the results reported in section 2.

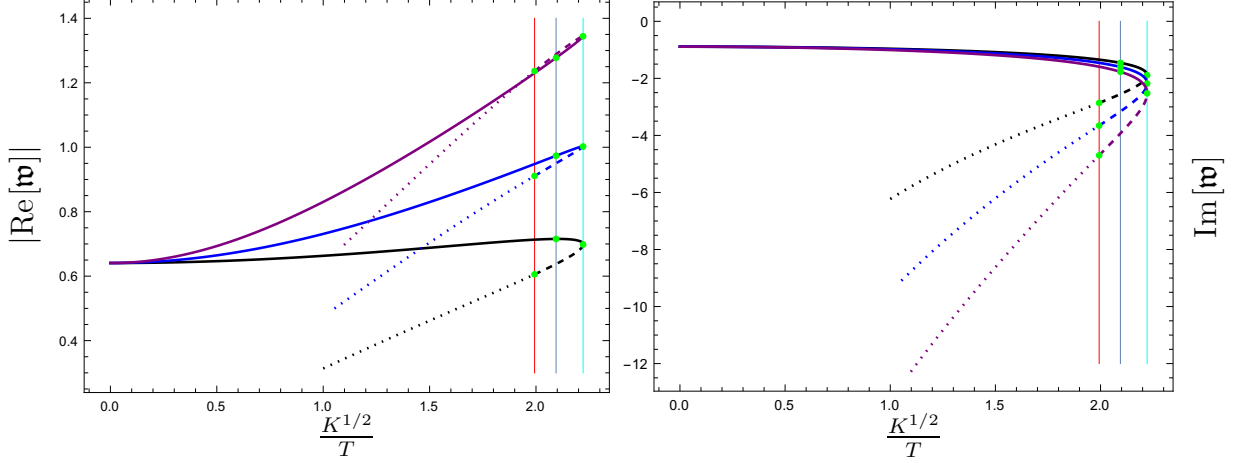


Figure 6:  $\text{Re}[\mathfrak{w}]$  (the left panel) and  $\text{Im}[\mathfrak{w}]$  (the right panel) of the lowest  $\Delta = 2$  QNMs in the disordered phase of  $\mathfrak{M}_{PW}$  model with  $\ell = 0$  (black curves),  $\ell = 1$  (blue curves) and  $\ell = 2$  (purple curves).

#### 4.1 $\mathfrak{M}_{PW}^b$ model in the limit $b \rightarrow +\infty$

Conformal order in the limit  $b \rightarrow +\infty$  becomes perturbative [9]. We can solve eqs. (A.6)-(A.8) as a series expansion in  $\frac{1}{b}$ :

$$\begin{aligned} \alpha(r) &= \sum_{n=1}^{\infty} \frac{1}{b^{2n-1}} \alpha_n(r), & h &= \frac{16}{(1+r)^4} \left( 1 + \sum_{n=1}^{\infty} \frac{1}{b^{2n}} h_n(r) \right), \\ f &= \frac{(2r+1)(16Kr^2 + 2r^2 + 2r + 1)}{(r+1)^4} \left( 1 + \sum_{n=1}^{\infty} \frac{1}{b^{2n}} f_n(r) \right), \end{aligned} \quad (4.1)$$

where we explicitly factor the  $AdS_5$ -Schwarzschild black brane/black hole solution in the strict  $b \rightarrow +\infty$  limit, see (3.4). To the leading  $n = 1$  order we find:

$$\begin{aligned} 0 = \alpha_1'' + \frac{32Kr^4 + 4r^4 - 16Kr^2 - 10r^2 - 10r - 3}{r(2r+1)((16K+1)r^2 + (r+1)^2)(r+1)} \alpha_1' \\ - \frac{4\alpha_1(r+1)^2(\alpha_1 - 1)}{((16K+1)r^2 + (r+1)^2)(2r+1)r^2}, \end{aligned} \quad (4.2)$$

$$0 = h_2'' + \frac{2}{r+1} h_2' - 16(\alpha_1')^2, \quad (4.3)$$



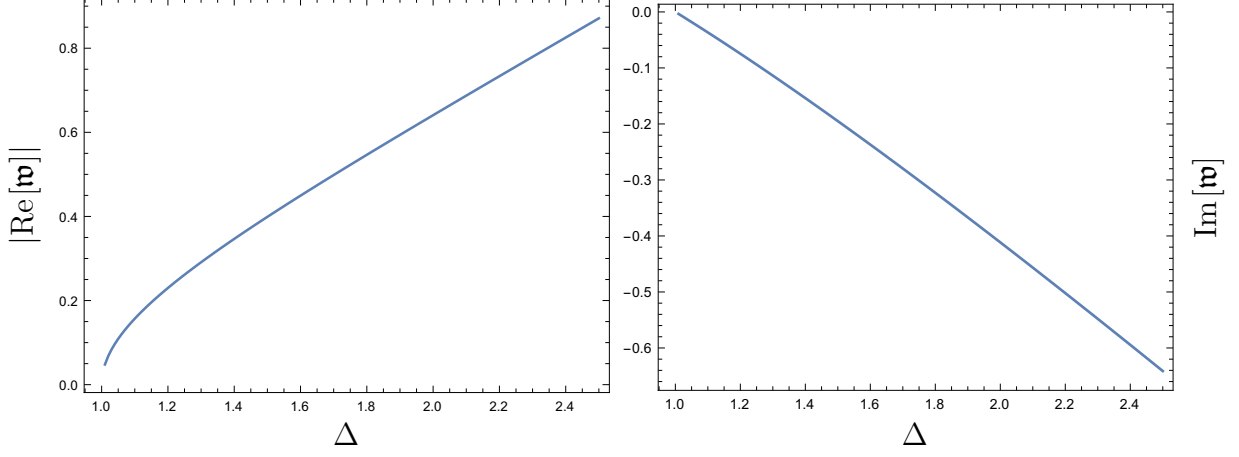


Figure 7:  $\text{Re}[\mathfrak{w}]$  (the left panel) and  $\text{Im}[\mathfrak{w}]$  (the right panel) of the lowest  $\ell = 0$  QNMs in the disordered phase with  $\Delta \in (1, \frac{5}{2})$ .

$$\begin{aligned}
0 = & f_2' + 4(r+1)r(\alpha_1')^2 - \frac{8Kr^4 + 48Kr^3 + r^4 + 24Kr^2 + 8r^3 + 12r^2 + 8r + 2}{(2r+1)(16Kr^2 + 2r^2 + 2r + 1)} h_2' \\
& - \frac{4(r+1)(8Kr^2 + r^2 + 2r + 1)}{(2r+1)(16Kr^2 + 2r^2 + 2r + 1)r} f_2 + \frac{2(r+1)(16Kr^2 + r^2 + 2r + 1)}{(2r+1)(16Kr^2 + 2r^2 + 2r + 1)r} h_2 \\
& - \frac{16(r+1)^3(2\alpha_1 - 3)\alpha_1^2}{3r(2r+1)(16Kr^2 + 2r^2 + 2r + 1)}.
\end{aligned} \tag{4.4}$$

Eqs. (4.2)-(4.4) are solved with the following asymptotics:

- in the UV, *i.e.*, as  $r \rightarrow 0$

$$\alpha_1 = \alpha_{1,2} r^2 + \mathcal{O}(r^3), \quad h_2 = \frac{16}{3} \alpha_{1,2}^2 r^4 + \mathcal{O}(r^5), \quad f_2 = f_{2,4} r^4 + \mathcal{O}(r^5), \tag{4.5}$$

- in the IR, *i.e.*, as  $y \equiv \frac{1}{r} \rightarrow 0$

$$\begin{aligned}
\alpha_1 = & \alpha_{1,0}^h + \mathcal{O}(y), \quad h_2 = h_{2,0}^h + h_{2,1}^h y + \mathcal{O}(y^2), \\
f_2 = & \frac{16(\alpha_{1,0}^h)^2(3 - 2\alpha_{1,0}^h) + 6h_{2,0}^h(16K + 1) + 3h_{2,1}^h(8K + 1)}{12(8K + 1)} + \mathcal{O}(y).
\end{aligned} \tag{4.6}$$

From (A.15) we find

$$\begin{aligned}
\hat{\mathcal{E}} = & \frac{3(8K + 1)^2}{256\pi^4 K^2} - \frac{3f_{2,4}}{256\pi^4 K^2} \frac{1}{b^2} + \mathcal{O}(b^{-4}), \quad \hat{s} = \frac{1}{16\pi^3 K^{3/2}} - \frac{3h_{2,0}^h}{64\pi^3 K^{3/2}} \frac{1}{b^2} + \mathcal{O}(b^{-4}), \\
\hat{T} = & \frac{8K + 1}{4\pi K^{1/2}} + \frac{16(\alpha_{1,0}^h)^2(3 - 2\alpha_{1,0}^h) + 48Kh_{2,0}^h + 3h_{2,1}^h(8K + 1)}{48\pi K^{1/2}} \frac{1}{b^2} + \mathcal{O}(b^{-4}).
\end{aligned} \tag{4.7}$$

The first law of thermodynamics at order  $\mathcal{O}(b^{-2})$  leads to the constraint

$$0 = \delta_{pert} \equiv 1 - \frac{2K(8K+1)}{h_{2,0}^h(3+8K)} (h_{2,0}^h)' + \frac{2K}{h_{2,0}^h(3+8K)} (f_{2,4})' - \frac{8K+1}{h_{2,0}^h(3+8K)} h_{2,1}^h - \frac{4}{h_{2,0}^h(3+8K)} f_{2,4} + \frac{16(\alpha_{1,0}^h)^2(2\alpha_{1,0}^h-3)}{3h_{2,0}^h(3+8K)}, \quad (4.8)$$

where  $'$  stands for  $\frac{d}{dK}$ . We verify the first law of thermodynamics of the conformal order at  $\mathcal{O}(b^{-2})$  in fig. 9.

We now discuss the computation of the QNMs in the perturbative conformal order. In the limit  $b \rightarrow +\infty$ , the differential operator  $\mathcal{D}_2$  in (B.2) is

$$\mathcal{D}_2 = \mathcal{D}_2 \Big|_{AdS_5-Schwarzschild} + \mathcal{O}(b^{-2}), \quad (4.9)$$

while  $W$  in (B.3) is

$$W = -1 + 2\alpha_1 + \mathcal{O}(b^{-2}). \quad (4.10)$$

Note that the highlighted term in  $W$  implies that the QNM spectra of the ordered and the disordered phases are different even in the strict  $b \rightarrow +\infty$  limit.

## 4.2 $\mathfrak{M}_{PW}^b$ model at finite $b$

Using the equations of motions and the asymptotics for the background and the QNMs in appendices A and B, the numerical solution is routine. We use the computation techniques developed in [29]. To validate numerical solutions we verify the first law (A.17). For example, for  $K=0$ , the first law can be stated as

$$0 = \delta_{K=0} \equiv \frac{4\hat{\mathcal{E}} - 3\hat{T}\hat{s}}{4\hat{\mathcal{E}}} - 1. \quad (4.11)$$

We present the results for  $\delta_{K=0}$  in fig. 9.

We conclude this section explaining how to obtain the results for  $b_{crit}$  reported in fig. 4. We focus on the red dot in the figure, representing the uncompactified ( $K=0$ ) conformal order in  $\mathfrak{M}_{PW}^b$  model. The background geometry representing the conformal order is determined by the set of parameters in the asymptotic expansions — see (A.10)-(A.13). Consider the parameter  $h_0^h$ . In the limit  $b \rightarrow +\infty$  we can use the  $AdS_5$ -Schwarzschild solution (3.4) to conclude (remember the redefinition (A.14))

$$\lim_{b \rightarrow +\infty} (h_0^h)^{-1} = \frac{1}{16}. \quad (4.12)$$

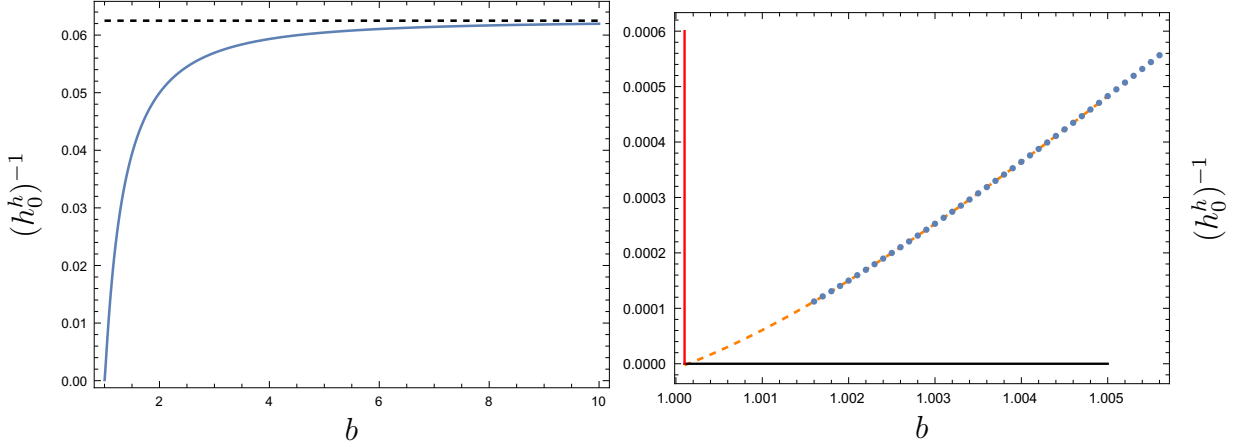


Figure 8: Computation of  $b_{crit}$  in  $\mathfrak{M}_{PW}^b$  model at  $K = 0$ . The IR parameter  $h_0^h$  (see (A.13)) determining the bulk solution diverges as  $b \rightarrow b_{crit}$ . We estimate the location of this divergence interpolating the small- $b$  data (the dashed orange curve in the right panel).

This asymptote is represented by a dashed black line in the left panel of fig. 8. As  $b$  decreases,  $h_0^h$  increases, ultimately diverging as  $b \rightarrow b_{crit}$ . Of course we can not reliably construct singular solutions — in the right panel of fig. 8 the points indicate values of  $(h_0^h)^{-1}$  for small  $b$ . We use Wolfram Mathematica interpolation (orange dashed curve) to estimate the location of the divergence of  $h_0^h$  (highlighted with the vertical red line).

### 4.3 $\mathfrak{M}_{PW,sym}^b$ model in the limit $b \rightarrow +\infty$

The perturbative expansion in  $\mathfrak{M}_{PW,sym}^b$  model takes form

$$\begin{aligned}
 \alpha(r) &= \sum_{n=1}^{\infty} \frac{1}{b^{n-1/2}} \alpha_n(r), & h &= \frac{16}{(1+r)^4} \left( 1 + \sum_{n=1}^{\infty} \frac{1}{b^n} h_n(r) \right), \\
 f &= \frac{(2r+1)(16Kr^2 + 2r^2 + 2r + 1)}{(r+1)^4} \left( 1 + \sum_{n=1}^{\infty} \frac{1}{b^n} f_n(r) \right).
 \end{aligned} \tag{4.13}$$

To reproduce the results reported in fig. 5 we need the equation for  $\alpha_1$ , and the leading order expression for  $W$  (computing the spectrum of the QNMs as in (B.1)):

$$\begin{aligned}
0 = & \alpha_1'' + \frac{16Kr^2(2r^2 - 1) + 4r^4 - 10r^2 - 10r - 3}{r(2r + 1)(16Kr^2 + 2r^2 + 2r + 1)(r + 1)} \alpha_1' \\
& + \frac{4\alpha_1(r + 1)^2(2\alpha_1^2 + 1)}{(16Kr^2 + 2r^2 + 2r + 1)(2r + 1)r^2}, \\
\alpha_1 = & \alpha_{1,2}r^2 + \mathcal{O}(r^3), \quad \alpha_1 = \alpha_{1,0}^h + \mathcal{O}(y),
\end{aligned} \tag{4.14}$$

and

$$W = -1 - 6\alpha_1^2 + \mathcal{O}(b^{-1}). \tag{4.15}$$

## Acknowledgments

This research is supported in part by Perimeter Institute for Theoretical Physics. Research at Perimeter Institute is supported in part by the Government of Canada through the Department of Innovation, Science and Economic Development Canada and by the Province of Ontario through the Ministry of Colleges and Universities. This work was further supported by NSERC through the Discovery Grants program.

## A Hairy black holes and their thermodynamics in $\mathfrak{M}_{PW}^b$ model

We parameterize black hole solutions in  $\mathfrak{M}_{PW}^b$  model as

$$ds_5^2 = -c_1^2 dt^2 + c_2^2 d\Omega_{(3,K)}^2 + c_3^2 dr^2, \quad \alpha = \alpha(r), \tag{A.1}$$

where the radial coordinate  $r$  ranges as

$$r \in (0, +\infty), \tag{A.2}$$

where  $c_i = c_i(r)$ ,

$$c_1 = \frac{f^{1/2}}{rh^{1/4}}, \quad c_2 = \frac{1}{rh^{1/4}}, \quad c_3 = \frac{h^{1/4}}{rf^{1/2}}, \tag{A.3}$$

and the round 3-sphere metric  $d\Omega_{(3,K)}^2$  of radius  $K^{-1/2}$  is

$$d\Omega_{3,K}^2 = \frac{dx^2}{(1 - Kx^2)} + (1 - Kx^2) \left[ \frac{dy^2}{(1 - Ky^2)} + (1 - Ky^2) dz^2 \right]. \tag{A.4}$$

From the gravitational effective Lagrangian of  $\mathfrak{M}_{PW}^b$  model (see (2.5) for the scalar potential)

$$\mathcal{L}_{\mathfrak{M}_{PW}^b} = R - 12(\partial\alpha)^2 - V_{\mathfrak{M}_{PW}^b}, \quad (\text{A.5})$$

we obtain the following second order equations:

$$0 = f'' - \frac{3f'}{r} - \frac{5h'f'}{4h} + 4hK, \quad (\text{A.6})$$

$$0 = h'' - \frac{5(h')^2}{4h} - 16h(\alpha')^2, \quad (\text{A.7})$$

$$0 = \alpha'' + a' \left( \frac{f'}{f} - \frac{3}{r} - \frac{5h'}{4h} \right) + \frac{h^{1/2}b}{6r^2f} (e^{2\alpha} - e^{-4\alpha}) + (1-b) \frac{h^{1/2}\alpha}{r^2f}, \quad (\text{A.8})$$

and the first order constraint

$$0 = (\alpha')^2 + \frac{hK}{2f} - \frac{(h')^2}{16h^2} + \frac{h'f'}{16fh} - \frac{h'}{2rh} + \frac{f'}{4rf} - \frac{1}{r^2} + \frac{h^{1/2}b}{6r^2f} \left( e^{2\alpha} + \frac{1}{2}e^{-4\alpha} \right) + (1-b) \frac{h^{1/2}\alpha^2}{r^2f}. \quad (\text{A.9})$$

Eqs. (A.6)-(A.9) are solved with the following asymptotics:

- in the UV, *i.e.*, as  $r \rightarrow 0$

$$f = 1 + 16Kr^2 - 32Kr^3 + f_4r^4 + \mathcal{O}(r^5), \quad (\text{A.10})$$

$$h = 16 - 64r + 160r^2 - 320r^3 + \left( 560 + \frac{256}{3}a_2^2 \right) r^4 + \mathcal{O}(r^5), \quad (\text{A.11})$$

$$\alpha = a_2r^2 - 2a_2r^3 + (a_2^2b + 3a_2)r^4 + \mathcal{O}(r^5), \quad (\text{A.12})$$

- in the IR, *i.e.*, as  $y \equiv \frac{1}{r} \rightarrow 0$

$$f = f_1^h y + \mathcal{O}(y^2), \quad \hat{h} = h_0^h + \mathcal{O}(y), \quad \alpha = a_0^h + \mathcal{O}(y), \quad (\text{A.13})$$

where we defined

$$\hat{h} \equiv y^{-4} h. \quad (\text{A.14})$$

Following the holographic renormalization of the related  $\mathcal{N} = 2^*$  model [30–32] we find:

$$\hat{\mathcal{E}} = \frac{1}{8\pi^4} \left( 6 + \frac{9}{2K} - \frac{3f_4}{32K^2} \right), \quad \hat{s} = \frac{1}{2\pi^3 (h_0^h)^{3/4} K^{3/2}}, \quad \hat{T} = \frac{f_1^h}{4\pi (h_0^h)^{1/2} K^{1/2}}. \quad (\text{A.15})$$

The basic thermodynamic relation,

$$\hat{\mathcal{F}} = \hat{\mathcal{E}} - \hat{s}\hat{T}, \quad (\text{A.16})$$

is automatically enforced by the holographic renormalization [31], while the first law of thermodynamics,

$$d\hat{\mathcal{E}} = \hat{T} d\hat{s} \Big|_{b=\text{const}}, \quad (\text{A.17})$$

must be verified numerically. We always check (A.17) in numerical constructions of  $\mathfrak{M}_{PW}^b$  model black hole geometries. See appendix C for a sample of such tests.

## B $h = 0$ QNMs of the hairy black holes in $\mathfrak{M}_{PW}^b$ model

We follow the framework of [13] for the computation of the QNMs. We will be interested in the helicity  $h = 0$  quasinormal modes with  $\ell = 0$ . Note that at  $\ell = 0$  the metric and the bulk scalar fluctuations decouple. We use  $F(t, r)$  to denote gauge invariant fluctuations associated with the bulk scalar  $\alpha$  of the conformal model  $\mathfrak{M}_{PW}^b$ . Using the background parameterization (A.3), we obtain from [13]:

$$0 = \mathcal{D}_2 F - W F, \quad (\text{B.1})$$

where the second-order differential operator  $\mathcal{D}_2$  (coming from  $\square$  on the background geometry (A.1)) is (note that  $k^2 = K\ell(\ell + 2) = 0$ )

$$\begin{aligned} \mathcal{D}_2 F(t, r) &\equiv -\frac{h^{1/2}r^2}{f} \partial_{tt}^2 F + \frac{r^2 f}{h^{1/2}} \partial_{rr}^2 F + \left( \frac{r^2 f'}{h^{1/2}} - \frac{5r^2 f h'}{4h^{3/2}} - \frac{3rf}{h^{1/2}} \right) \partial_r F - h^{1/2}r^2 k^2 F \\ &= -\frac{h^{1/2}r^2}{f} \partial_{tt}^2 F + \frac{r^2 f}{h^{1/2}} \partial_{rr}^2 F + \left( \frac{r^2 f'}{h^{1/2}} - \frac{5r^2 f h'}{4h^{3/2}} - \frac{3rf}{h^{1/2}} \right) \partial_r F, \end{aligned} \quad (\text{B.2})$$

and

$$\begin{aligned} W &= \frac{1}{3hG^2} \left( 1536h^{5/2}fr^4(\alpha')^4 + 96h^{1/2}r^2(h'r + 4h)(hf'r - 4hf - h'fr)(\alpha')^2 \right. \\ &\quad \left. + 32\alpha'(h'r + 4h)(6\alpha h^2 r(1-b) + h^2 r b(e^{2\alpha} - e^{-4\alpha})) \right) - \frac{b}{3}(e^{2\alpha} + 2e^{-4\alpha}) + b - 1, \end{aligned} \quad (\text{B.3})$$

with

$$G \equiv h'r + 4h. \quad (\text{B.4})$$

Generically,  $F$ , as well as  $\mathfrak{w}$ , are complex. We need to impose the normalizable boundary conditions as  $r \rightarrow 0$ , and the incoming wave boundary conditions at the black brane/black hole horizon, *i.e.*, as  $y \equiv \frac{1}{r} \rightarrow 0$ . We can explicitly factor the boundary conditions, and the harmonic time dependence, redefining  $F$  as

$$F(t, r) = (1 + r)^{i\mathfrak{w}/2} \frac{r^2}{1 + r^2} e^{-i2\pi T\mathfrak{w}t} f(r), \quad (\text{B.5})$$

which renders  $f(r)$  regular and  $\mathcal{O}(1)$  both at the boundary and at the horizon.

Turns out that the unstable QNMs have  $\text{Im}[f] = 0$  and  $\text{Re}[\mathfrak{w}] = 0$ . Further introducing

$$f = f_{\text{Re}}, \quad \mathfrak{w} = i \mathfrak{w}_{\text{Im}}, \quad (\text{B.6})$$

we obtain from (B.1) a single second order linear ODEs for the real function  $f_{\text{Re}}$ . Because of the linearity, there is an arbitrary overall normalization of a solution; we fix this normalization imposing

$$\lim_{r \rightarrow 0} f_{\text{Re}} = 1. \quad (\text{B.7})$$

The QNM equation for  $f_{\text{Re}}$  is solved with the following asymptotics:

- in the UV, *i.e.*, as  $r \rightarrow 0$

$$f_{\text{Re}} = 1 + \left( -2 + \frac{1}{2} \mathfrak{w}_{\text{Im}} \right) r + \mathcal{O}(r^2), \quad (\text{B.8})$$

- in the IR, *i.e.*, as  $y \equiv \frac{1}{r} \rightarrow 0$

$$f_{\text{Re}} = f_{\text{Re},0}^h + \mathcal{O}(y). \quad (\text{B.9})$$

Note that, for a fixed background, the solution is characterized in total by 2 parameters

$$\{ \mathfrak{w}_{\text{Im}}, f_{\text{Re},0}^h \}, \quad (\text{B.10})$$

precisely as needed to specify a solution of a single second order ODE.

## C Numerical tests

In fig. 9 we test the first law of thermodynamics (A.17) for the perturbative conformal order (see (4.8), the left panel) and for the conformal order at  $K = 0$  (see (4.11), the right panel) in  $\mathfrak{M}_{PW}^b$  model.

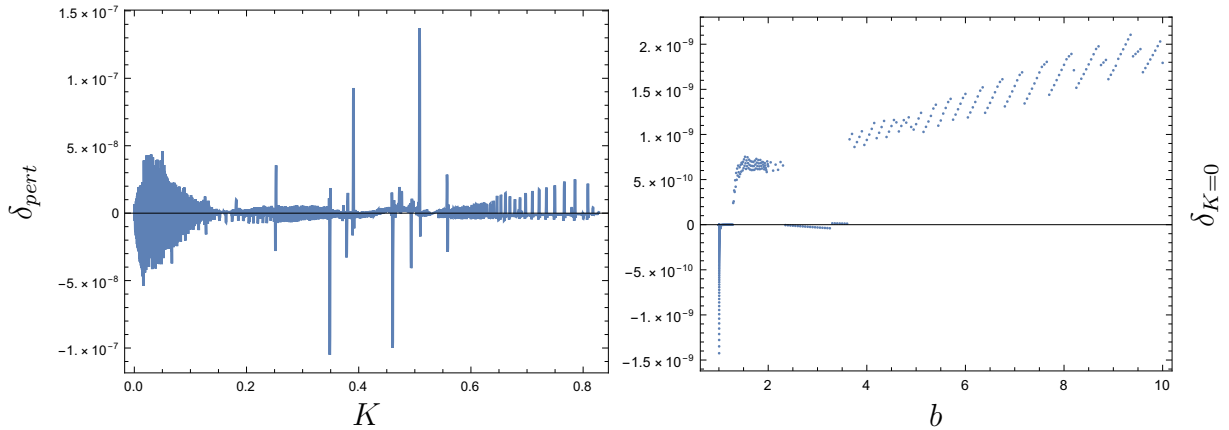


Figure 9: Numerical tests of the first law of thermodynamics for the perturbative conformal order (the left panel) and the conformal order at  $K = 0$  (the right panel) in  $\mathfrak{M}_{PW}^b$  model.

## References

- [1] N. Chai, S. Chaudhuri, C. Choi, Z. Komargodski, E. Rabinovici and M. Smolkin, *Thermal Order in Conformal Theories*, *Phys. Rev. D* **102** (2020) 065014, [2005.03676].
- [2] S. Chaudhuri, C. Choi and E. Rabinovici, *Thermal order in large  $N$  conformal gauge theories*, *JHEP* **04** (2021) 203, [2011.13981].
- [3] N. Chai, A. Dymarsky and M. Smolkin, *A model of persistent breaking of discrete symmetry*, 2106.09723.
- [4] S. Chaudhuri and E. Rabinovici, *Symmetry breaking at high temperatures in large  $N$  gauge theories*, 2106.11323.
- [5] J. M. Maldacena, *The Large  $N$  limit of superconformal field theories and supergravity*, *Int. J. Theor. Phys.* **38** (1999) 1113–1133, [hep-th/9711200].
- [6] O. Aharony, S. S. Gubser, J. M. Maldacena, H. Ooguri and Y. Oz, *Large  $N$  field theories, string theory and gravity*, *Phys. Rept.* **323** (2000) 183–386, [hep-th/9905111].
- [7] A. Buchel and C. Pagnutti, *Exotic Hairy Black Holes*, *Nucl. Phys. B* **824** (2010) 85–94, [0904.1716].



- [8] A. Buchel, *Thermal order in holographic CFTs and no-hair theorem violation in black branes*, *Nucl. Phys. B* **967** (2021) 115425, [2005.07833].
- [9] A. Buchel, *SUGRA/Strings like to be bald*, *Phys. Lett. B* **814** (2021) 136111, [2007.09420].
- [10] A. Buchel, *Klebanov-Strassler black hole*, *JHEP* **01** (2019) 207, [1809.08484].
- [11] A. Buchel, *A bestiary of black holes on the conifold with fluxes*, 2103.15188.
- [12] A. Buchel, *Fate of the conformal order*, *Phys. Rev. D* **103** (2021) 026008, [2011.11509].
- [13] A. Buchel, *Stabilization of the extended horizons*, 2105.13380.
- [14] K. Pilch and N. P. Warner,  *$N=2$  supersymmetric RG flows and the IIB dilaton*, *Nucl. Phys.* **B594** (2001) 209–228, [hep-th/0004063].
- [15] A. Buchel, A. W. Peet and J. Polchinski, *Gauge dual and noncommutative extension of an  $N=2$  supergravity solution*, *Phys.Rev.* **D63** (2001) 044009, [hep-th/0008076].
- [16] A. Buchel, J. G. Russo and K. Zarembo, *Rigorous Test of Non-conformal Holography: Wilson Loops in  $N=2^*$  Theory*, *JHEP* **03** (2013) 062, [1301.1597].
- [17] N. Bobev, H. Elvang, D. Z. Freedman and S. S. Pufu, *Holography for  $N = 2^*$  on  $S^4$* , *JHEP* **07** (2014) 001, [1311.1508].
- [18] A. Buchel, S. Deakin, P. Kerner and J. T. Liu, *Thermodynamics of the  $N=2^*$  strongly coupled plasma*, *Nucl. Phys. B* **784** (2007) 72–102, [hep-th/0701142].
- [19] C. Hoyos, S. Paik and L. G. Yaffe, *Screening in strongly coupled  $N=2^*$  supersymmetric Yang-Mills plasma*, *JHEP* **10** (2011) 062, [1108.2053].
- [20] S. W. Hawking and D. N. Page, *Thermodynamics of Black Holes in anti-De Sitter Space*, *Commun. Math. Phys.* **87** (1983) 577.
- [21] E. Witten, *Anti-de Sitter space, thermal phase transition, and confinement in gauge theories*, *Adv. Theor. Math. Phys.* **2** (1998) 505–532, [hep-th/9803131].

- [22] V. E. Hubeny and M. Rangamani, *Unstable horizons*, *JHEP* **05** (2002) 027, [[hep-th/0202189](#)].
- [23] A. Buchel and L. Lehner, *Small black holes in  $AdS_5 \times S^5$* , *Class. Quant. Grav.* **32** (2015) 145003, [[1502.01574](#)].
- [24] A. Ishibashi and H. Kodama, *Stability of higher dimensional Schwarzschild black holes*, *Prog. Theor. Phys.* **110** (2003) 901–919, [[hep-th/0305185](#)].
- [25] A. Buchel, *Universality of small black hole instability in AdS/CFT*, *Int. J. Mod. Phys. D* **26** (2017) 1750140, [[1509.07780](#)].
- [26] P. Breitenlohner and D. Z. Freedman, *Stability in Gauged Extended Supergravity*, *Annals Phys.* **144** (1982) 249.
- [27] I. R. Klebanov and E. Witten, *AdS / CFT correspondence and symmetry breaking*, *Nucl. Phys. B* **556** (1999) 89–114, [[hep-th/9905104](#)].
- [28] G. T. Horowitz and V. E. Hubeny, *Quasinormal modes of AdS black holes and the approach to thermal equilibrium*, *Phys. Rev. D* **62** (2000) 024027, [[hep-th/9909056](#)].
- [29] O. Aharony, A. Buchel and P. Kerner, *The Black hole in the throat: Thermodynamics of strongly coupled cascading gauge theories*, *Phys. Rev.* **D76** (2007) 086005, [[0706.1768](#)].
- [30] A. Buchel, *Black hole spectra in holography: consequences for equilibration of dual gauge theories*, *Nucl. Phys. B* **896** (2015) 587–610, [[1501.04593](#)].
- [31] A. Buchel,  *$N=2^*$  hydrodynamics*, *Nucl. Phys. B* **708** (2005) 451–466, [[hep-th/0406200](#)].
- [32] A. Buchel, L. Lehner and R. C. Myers, *Thermal quenches in  $N=2^*$  plasmas*, *JHEP* **08** (2012) 049, [[1206.6785](#)].